Available online at www.sciencedirect.com
ScienceDirect
Trans. Nonferrous Met. Soc. China 25(2015) 1043−1049
Transactions of Nonferrous Metals Society of China
www.tnmsc.cn

Springback and tensile strength of 2A97 aluminum alloy during age forming

Hong-ying LI, Xiao-chao LU

School of Materials Science and Engineering, Central South University, Changsha 410083, China

Received 7 January 2014; accepted 17 December 2014

Abstract: The analysis of variance (ANOVA), multiple quadratic regression and radial basis function artificial neural network (RBFANN) methods were used to study the springback and tensile strength in age forming of 2A97 aluminum alloy based on orthogonal array. The ANOVA analysis indicates that the springback reaches the minimum value when age forming is performed at 210 °C for 20 h using a single-curvature die with a radius of 400 mm, and the tensile strength reaches the maximum value when age forming is performed at 180 °C for 15 h using a single-curvature die with a radius of 1000 mm. The orders of the importance for the three factors of pre-deformation radius, aging temperature and aging time on the springback and tensile strength were determined. By analyzing the predicted results of the multiple quadratic regression and RBFANN methods, the prediction accuracy of the RBFANN model is higher than that of the regression model.

Key words: aluminum alloy; age forming; springback; tensile strength; orthogonal experiment; artificial neural network

1 Introduction

Al−Li alloys have been widely applied in aircraft manufacturing due to their low density, high elastic modulus and high specific strength [1,2]. 2A97 alloy was developed primarily in an attempt to be used for plates and forgings as a promising aerospace material [3]. However, there are some limits in forming integral aircraft wing panels by traditional forming techniques (such as brake forming, roll forming and shot peen forming) due to their poor assembling ability and the increase of mass. Therefore, a new forming technique is a key for 2A97 alloys to be used to manufacture complex-shaped panel parts. Age forming technique has then been regarded for it can form large integrally stiffened light mass structures [4,5].

Age forming, combining both the aging treatment and forming process, is currently applied to the production of aerospace metal structures. And it has been proven to be very useful for forming components with these shape characteristics and good mechanical properties [6,7]. One of the greatest challenges to improve the efficiency of the age forming technique is to predict the exact amount of springback that will arise, in order that a tool shape may be defined to compensate for it. While in age forming process, springback can be influenced by many parameters, such as aging temperature, aging time and pre-deformation radius. The prediction of the ultimate mechanical properties is also necessary for optimizing the process schedule of age forming. The predictive model can be created using the regression and artificial neural network (ANN) methods based on orthogonal array. Orthogonal design is a method for test design aiming to multifactor and multilevel based on orthogonal theory. Since it presents equilibrium distribution and regular comparability, the optimum scheme can be rapidly obtained by analysis of variance, largely reducing testing number, shortening test time, and minimizing cost. The regression method has successfully been used for obtaining the machining performance by many researchers [8,9]. On the other hand, the ANN has the ability to approximate many functions accurately and hence is suitable for the use in model development of highly non-linear processes. Unlike the regression methods, an artificial neural network does not need to postulate a mathematical model or identify its parameters [10,11]. The ANN learns from training data and recognizes patterns in a series of input and output values without any prior assumptions about their nature and interrelations [12]. They have been successfully applied to solving many practical problems [13,14].

However, the study about the age forming of 2A97

Corresponding author: Hong-ying LI; Tel: +86-731-88836328; E-mail: lhying@csu.edu.cn
DOI: 10.1016/S1003-6326(15)63696-2

aluminum alloy has not been found. It is of great significance to determine the relationship between the two parameters (springback and tensile strength) and the three factors (pre-deformation radius, aging temperature and aging time) in age forming of 2A97 aluminum alloy. In the present work, the analysis of variance (ANOVA), multiple quadratic regression and radial basis function artificial neural network (RBFANN) methods were carried out based on orthogonal array. And the prediction capacities of the multiple quadratic regression and RBFANN models were compared.

2 Experimental

2.1 Materials and procedures

The experiments were carried out on a 2A97 alloy rolled plate with composition (mass fraction) of 3.7% Cu, 1.5% Li, 0.50% Zn, 0.37% Mg, 0.30% Mn, 0.14% Zr and balance Al. Sheet specimens with dimensions of 400 mm × 80 mm × 1.5 mm were used for age forming tests. All specimens under as-received conditions were solution treated at 520 °C for 1.5 h before water quenched to room temperature, and the transfer time must be less than 15 s. Then, the processed samples were kept under a refrigerated condition to prevent from natural aging. In the end, age forming was performed under controlled conditions of temperature and time, using single-curvature dies with different radii. The bended direction was along the rolling direction. The experimental procedures are shown in Fig. 1.

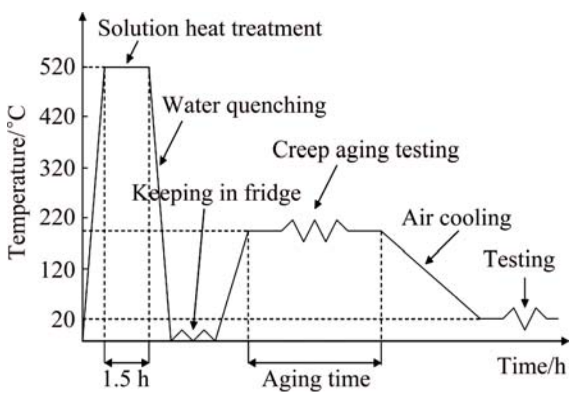

Fig. 1 Material preparation and test program

The amount of springback (S_P) is defined by

$$S_P = \frac{R_f - R_0}{R_f} \times 100\% \quad (1)$$

where R_f is the radius after springback, and R_0 is pre-deformation radius. S_P=0 indicates the absence of springback, and S_P=1 indicates a complete springback of the plate.

Tensile tests were carried out according to ASTM standard E−8M to evaluate the mechanical properties of the samples. The tensile samples were machined directly from the sheets after age forming. The samples were taken in the longitudinal (L) orientation (parallel to the rolling direction). The gauge length was 60 mm. These samples were stretched at room temperature and a constant extension rate of 1 mm/min. Three tensile tests were performed for every specimen to ensure the reproducibility of the tensile results.

2.2 Experimental design

In the experimental plan, the factors selected as controllable ones in this work were the pre-deformation radius (R_0), aging temperature (θ) and aging time (t), and four levels for each factor were selected. The factors and levels are tabulated in Table 1. Normally, one needs to conduct 4^3(64) experiments with three factors, and each varies at four levels considered, using full factorial experimental design. In order to save experimental cost and time, orthogonal array was applied to obtaining the springback (S_P) and tensile strength (R_m) of the specimen after age forming. An L_{16} (4^3) orthogonal array was found to be appropriate and was chosen in this work. The layout of the L_{16} (4^3) orthogonal array and the measured values of the S_P and R_m are shown in Table 2.

Table 1 Assignment of levels to factors

Level	R_0 (A)/mm	θ(B)/°C	t(C)/h
1	400	120	5
2	600	150	10
3	800	180	15
4	1000	210	20

Table 2 Orthogonal array L_{16} (4^3) and experimental results

Test No.	Level			S_P/%	R_m/MPa
	A	B	C		
1	1	1	1	59.104	389.54
2	1	2	2	47.862	443.46
3	1	3	3	30.683	509.14
4	1	4	4	9.674	453.75
5	2	1	2	56.033	419.39
6	2	2	1	59.673	412.42
7	2	3	4	31.034	512.59
8	2	4	3	16.704	473.78
9	3	1	3	54.883	449.49
10	3	2	4	48.262	481.23
11	3	3	1	58.502	471.89
12	3	4	2	29.364	509.14
13	4	1	4	57.334	464.58
14	4	2	3	54.753	487.08
15	4	3	2	47.703	527.17
16	4	4	1	50.731	487.57

3 Results and discussion

3.1 Analysis of variance (ANOVA)

An ANOVA of the data was done with the springback and the tensile strength for analyzing the influence of the pre-deformation radius, aging temperature and aging time of the contact on the total variance of the results, respectively. Tables 3 and 4 show the results of the ANOVA with the springback and tensile strength, respectively. The last columns of Tables 3 and 4 show the percentage of contribution (P) of each factor to the total variation indicating the degree of influence on the result. From Table 3, we can observe that factor B, the aging temperature, with ontribution of 56.49%, has the greatest influence on the springback. The relative influence of the factors on the springback was in the following order: aging temperature > aging time > pre-deformation radius.

Table 3 Analysis of variance for springback test

Source of variance	Deviation	Degree of freedom	Variance	Test F	P/%
A	595.0114	3	198.3371	23.91	14.96
B	2178.2628	3	726.0876	87.53	56.49
C	988.6978	3	329.5659	39.73	25.29
Error	49.7720	6	8.2950	−	3.26
Total	38811.7440	15	−	−	100

Table 4 Analysis of variance for tension test

Source of variance	Deviation	Degree of freedom	Variance	Test F	P/%
A	4794.07	3	1598.03	7.53	18.38
B	12337.46	3	4112.49	19.39	51.75
C	4207.12	3	1402.37	6.61	15.80
Error	1272.83	6	212.138	−	14.07
Total	22611.48	15	−	−	100

From Table 4, it can be observed that the percentage of contribution (P=51.75%) of factor B, the aging temperature, is much larger compared with that for the other two factors, viz., the pre-deformation radius and aging time. The relative influence of the factors on the tensile strength is in the following order: aging temperature >> pre-deformation radius > aging time.

The performance of the individual factor (the pre-deformation radius, aging temperature and aging time) at different levels for the springback (S_P) and tensile strength (R_m) is depicted in Fig. 2. It can be seen from Fig. 2(a) that the springback and tensile strength constantly increase with the increase of pre-deformation radius. As for the factor of the aging temperature in Fig. 2(b), the increase of the aging temperature leads to a significant decrease of the springback. The tensile strength increases with the increase of the aging temperature, reaches the maximum value at the aging temperature of 180 °C, and then decreases. It can be seen from Fig. 2(c) that the springback constantly decreases with the increase of aging time, and the tensile strength increases at first and then decreases with the increase of aging time. It can be found that the springback reaches the maximum at the pre-deformation radius of 1000 mm, aging temperature of 120 °C and aging time of 5 h, respectively, and the tensile strength reaches the

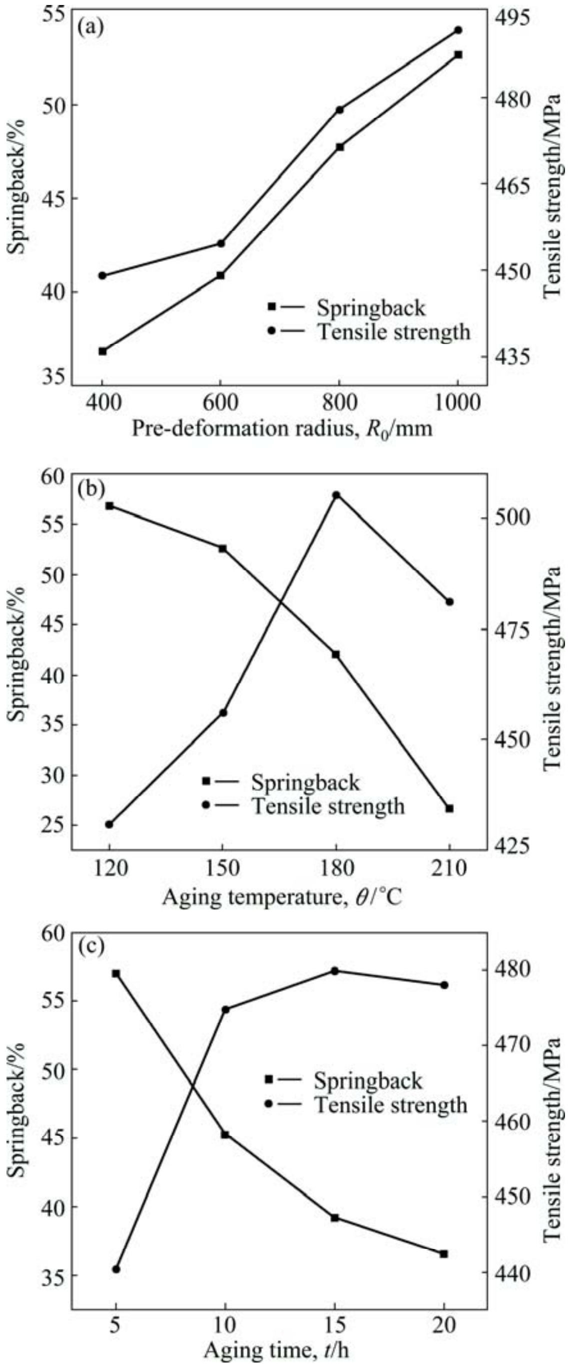

Fig. 2 Performance of individual factor at different levels for springback and tensile strength: (a) Pre-deformation radius; (b) Aging temperature; (c) Aging time

maximum value at the pre-deformation radius of 1000 mm, aging temperature of 180 °C and aging time of 15 h, respectively. Therefore, it can be concluded that the springback reaches the minimum value when age forming is performed at 210 °C for 20 h using a single-curvature die with a radius of 400 mm and the tensile strength specimen reaches the maximum value when age-forming is performed at 180 °C for 15 h using a single-curvature die with a radius of 1000 mm.

3.2 Regression analysis

The correlations between the factors (pre-deformation radius, aging temperature and aging time) and the measured parameters (the springback and tensile strength) were obtained by multiple quadratic regressions, respectively. The equations obtained are as follows:

$$S_P=0.013R_0+0.783\theta-0.743t+5.297\times10^{-6}R_0^2-0.03\theta^2+0.091t^2+5.608\times10^{-5}R_0\theta-0.013\theta t-0.001R_0t+12.149,\quad R=0.996 \tag{2}$$

$$R_m=-0.249R_0+4.685\theta+21.245t+5.056\times10^{-5}R_0^2-0.014\theta^2-0.363t^2+0.001R_0\theta-0.044\theta t-0.001R_0t-31.822,\quad R=0.897 \tag{3}$$

In order to confirm the verification of regression model, the comparison was done between the predicted values from the regression models (Eqs. (2) and (3)), with the values obtained experimentally. The errors calculated with respect to the calculated results were also given. The results are shown in Tables 5 and 6. It is clear that the errors of experimental results with respect to the

Table 5 Comparison of RBFANN and regression model results for springback with experimental values

Test No.	Level			Actual S_P/%	Predicted S_P by RBFANN/%	Error by RBFANN/%	Predicted S_P by Eq. (2)/%	Error by Eq. (2)/%
	A	*B*	*C*					
1	1	1	1	59.104	59.101	0.005	60.41	2.22
2	1	2	2	47.862	47.860	0.004	49.68	3.80
3	1	3	3	30.683	30.684	0.004	34.20	11.47
4	1	4	4	9.674	9.674	0.003	10.98	13.55
5	2	1	2	56.033	56.031	0.004	56.72	1.23
6	2	2	1	59.673	59.671	0.003	62.66	5.01
7	2	3	4	31.034	31.033	0.004	34.39	10.83
8	2	4	3	16.704	16.703	0.004	20.43	22.34
9	3	1	3	54.883	54.881	0.003	56.01	2.06
10	3	2	4	48.262	48.263	0.003	49.16	1.87
11	3	3	1	58.502	58.504	0.004	60.61	3.61
12	3	4	2	29.364	29.365	0.002	33.86	15.33
13	4	1	4	57.334	57.333	0.002	58.28	1.66
14	4	2	3	54.753	54.750	0.005	53.89	1.57
15	4	3	2	47.703	47.700	0.006	52.55	10.17
16	4	4	1	50.731	50.733	0.003	54.26	6.96

Table 6 Comparison of RBFANN and regression model results for tensile strength with experimental values

Test No.	Level			Actual R_m/MPa	Predicted R_m by RBFANN/MPa	Error by RBFANN/%	Predicted R_m by Eq. (3)	Error by Eq. (2)/%
	A	*B*	*C*					
1	1	1	1	389.54	389.59	0.006	354.02	9.12
2	1	2	2	443.46	443.45	0.001	430.57	2.91
3	1	3	3	509.14	509.12	0.004	450.57	11.50
4	1	4	4	453.75	453.76	0.003	414.02	8.76
5	2	1	2	419.39	419.38	0.002	386.93	7.74
6	2	2	1	412.42	412.43	0.003	375.88	8.86
7	2	3	4	512.59	512.61	0.004	443.98	13.39
8	2	4	3	473.78	473.78	0.004	418.83	11.60
9	3	1	3	449.49	449.51	0.005	403.74	10.18
10	3	2	4	481.23	481.25	0.005	440.79	8.40
11	3	3	1	471.89	471.90	0.003	388.59	17.65
12	3	4	2	509.14	509.15	0.002	411.54	19.17
13	4	1	4	464.58	464.57	0.002	404.44	12.95
14	4	2	3	487.08	487.06	0.004	430.49	11.62
15	4	3	2	527.17	527.20	0.006	426.39	19.12
16	4	4	1	487.57	487.56	0.002	392.14	19.57

calculated ones lie in the range of 1.23%−22.34% for the springback, 2.91%−19.57% for the tensile strength.

3.3 Artificial neural network

Artificial neural networks (ANNs) are the best known methods for solving non-linear problems. Their potential has been investigated with topics ranging from image processing and speech recognition to financial forecasting, as well as with material processing [14,15]. Among neural networks, the most popular one is the multilayer feed-forward net with the back-propagation areificial neural network (BPANN) learning algorithm. Recently, the radial basis function artificial neural network (RBFANN) model has been noted for its simple network structure that avoids lengthy calculations as compared with the BPANN, and has good robustness, as well as improved sensitivity to noisy data. In this work, the values of orthogonal arrays in Table 2 have been used to construct the RBFANN model. Two RBFANN models were established with three inputs (pre-deformation radius, aging temperature and aging time) and one output (either springback or tensile strength) for the prediction of springback and tensile strength, respectively. Before the training of the network, both input and output variables should be normalized within the range from 0 to 1 in order to obtain a usable form for the network to read. The following equation was used widely for unification:

$$x' = 0.1 + 0.8\frac{x - x_{\min}}{x_{\max} - x_{\min}} \tag{4}$$

where x is the original data, x' is the unified data of the corresponding x, $x_{\min}$ and $x_{\max}$ are the minimum and maximum values of x, respectively.

The parameter S_{PREAD} is a unique parameter which needs to be determined for establishing reliable RBFANN models of the springback or tensile strength, respectively. According to the experience, the parameter S_{PREAD}=2 was selected for the springback and S_{PREAD}=10 was selected for the tensile strength.

In order to confirm the verification of two RBFANN models, the comparison was done between the predicted values from the two RBFANN models, with the values obtained experimentally. The errors calculated with respect to the calculated results are also given (Tables 5 and 6). It is clear that the errors of the springback and tensile strength for the RBFANN are very small. Furthermore, other four tests were performed for investigating the prediction capacity of RBFANN model. The four experiment test data and the corresponding values predicted by RBFANN models as well as the errors are listed in Table 7. It can be seen that the error is very low, which shows that the well-trained RBFANN model has a great accuracy in predicting the springback and tensile strength.

3.4 Comparison between RBFANN and regression results

From Tables 5 and 6, we can observe that the test errors for the RBFANN model are lower than those of the regression model. This indicates that the RBFANN model is more suitable for estimating the springback and tensile strength in an acceptable error range. Furthermore, for the comparison of the prediction capacity of the RBFANN model and regression model, Fig. 3 shows the simulation variation of the springback and tensile strength as a function of the pre-deformation radius by the regression model and RBFANN model at θ=120 °C and t=10 h; θ=150 °C and t=20 h; θ=180 °C and t=15 h; θ=210 °C and t=5 h, respectively. Figure 4 shows the simulation variation of the springback and tensile strength as a function of the aging temperature by the regression model and RBFANN model at R_0=400 mm and t=20 h; R_0=600 mm and t=15 h; R_0=800 mm and t=5 h; R_0=1000 mm and t=10 h, respectively. Figure 5 shows the simulation variation of the springback and tensile strength as a function of the aging time by the regression model and RBFANN model at R_0=400 mm and θ=150 °C; R_0=600 mm and θ=180 °C; R_0=800 mm and θ=210 °C; R_0=1000 mm and θ=120 °C, respectively. From Figs. 3−5, most of the simulation results deviate from the experimental values. Nevertheless, the simulation results of the RBFANN models are in good agreement with the experimental results under all the conditions. This indicates that the prediction accuracy of the RBFANN model is higher than that of the regression model.

Table 7 Results of experiment tests and predictions by RBFANN

Test No.	Level			Actual S_P/%	Predicted S_P by RBFANN/%	Error of S_P / %	Actual R_m/MPa	Predicted R_m by RBFANN/MPa	Error of R_m/%
	A	B	C						
1	1	2	4	35.66	34.76	2.52	513.28	515.07	0.35
2	2	3	3	34.78	34.80	0	524.72	527.20	0.47
3	3	4	1	48.03	48.21	0.38	448.57	446.79	0.40
4	4	1	2	60.03	59.50	0.88	383.61	380.35	0.85

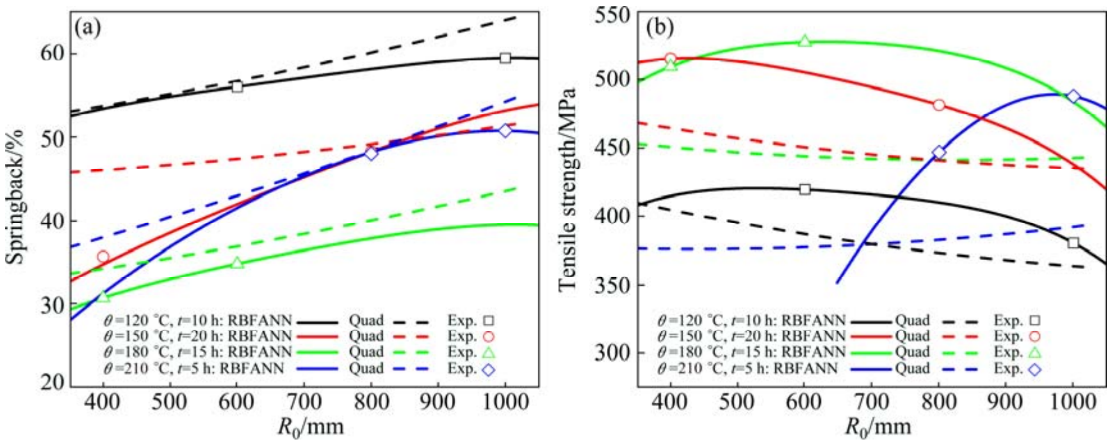

Fig. 3 Simulation variation of springback (a) and tensile strength (b) as function of pre-deformation radius by regression model and RBFANN model, respectively

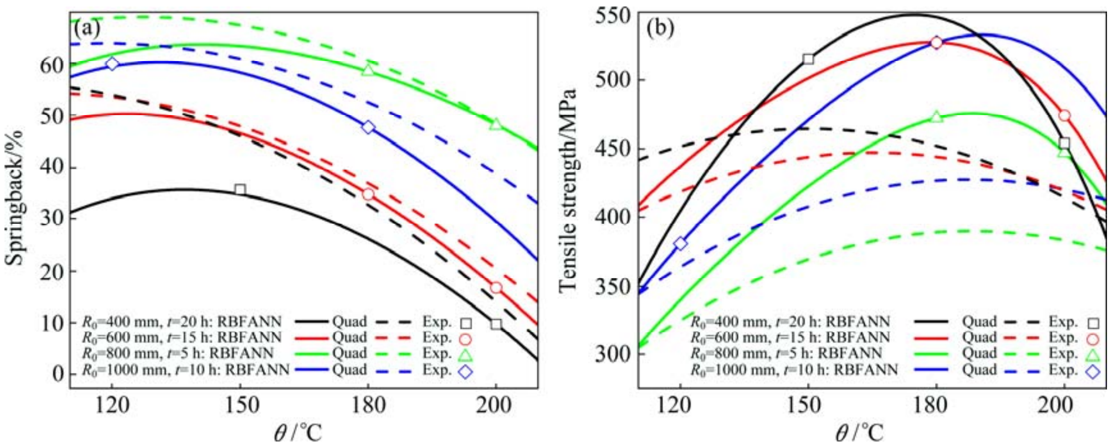

Fig. 4 Simulation variation of springback (a) and tensile strength (b) as function of aging temperature by regression model and RBFANN model, respectively

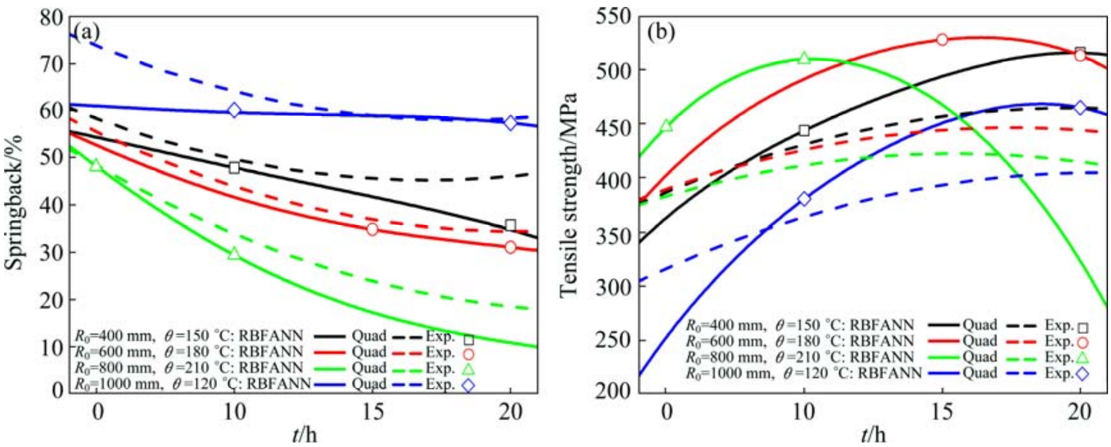

Fig. 5 Simulation variation of springback (a) and tensile strength (b) as function of aging time by regression model and RBFANN model, respectively

4 Conclusions

1) The ANOVA indicates that the springback reaches the minimum value under age forming conditions of 210 °C for 20 h using a single-curvature die with a radius of 400 mm and the tensile strength reaches the maximum value at under age-forming conditions of 180 °C for 15 h using a single-curvature die with a radius of 1000 mm.

2) The importance order for the factors to the springback, in sequence, is the aging temperature, the aging time, and the pre-deformation radius. The importance order to the tensile strength, in sequence, is the aging temperature, the pre-deformation radius and the aging time.

3) Both the regression and RBFANN methods can be used to obtain the model; however, the predicted results of the RBFANN models are in better agreement with the experimental results under any conditions. This indicates that the prediction accuracy of the RBFANN model is higher than that of the regression model.

References

[1] BENYELLOUL K, AOURAG H. Elastic constants of austenitic stainless steel: Investigation by the first-principles calculations and the artificial neural network approach [J]. Computational Materials Science, 2013, 67: 353−358.

[2] MUÑOZ-MORRIS M A, MORRIS D G. Microstructure control during severe plastic deformation of Al−Cu−Li and the influence on strength and ductility [J]. Materials Science and Engineering A, 2011, 528(9): 3445−3454.

[3] YUAN Zhi-shan, LU Zheng, XIE You-hua, WU Xiu-liang, DAI Sheng-long, LIU Chang-sheng. Mechanical properties of a novel high-strength aluminum−lithium alloy [J]. Materials Science Forum, 2011, 689: 385−389.

[4] ZHAN Li-hua, LI Yan-guang, HUANG Ming-hui, LIN Jian-guo. Comparative study of creep and stress relaxation behavior for 7055 aluminum alloy [J]. Advanced Materials Research, 2011, 314: 772−777.

[5] HOLMAN M C. Autoclave age forming large aluminum aircraft panels [J]. Journal of Mechanical Working Technology, 1989, 20: 477−488.

[6] ZHAN Li-hua, LIN Jian-guo, DEAN T A. A review of the development of creep age forming: Experimentation, modelling and applications [J]. International Journal of Machine Tools and Manufacture, 2011, 51(1): 1−17.

[7] ZHAN Li-hua, LI Yan-guang, HUANG Ming-hui. Effect of process parameters on microstructures of 7055 aluminum alloy in creep age forming [J]. Applied Mechanics and Materials, 2011, 80: 40−45.

[8] GUO Zhi-hong, HOU Hua, ZHAO Yu-hong, QU Shu-wei. Optimization of AZ80 magnesium alloy squeeze cast process parameters using morphological matrix [J]. Transactions of Nonferrous Metals Society of China, 2012, 22(2): 411−418.

[9] BADKAR D S, PANDEY K S, BUVANASHEKARAN G. Effects of laser phase transformation hardening parameters on heat input and hardened-bead profile quality of unalloyed titanium [J]. Transactions of Nonferrous Metals Society of China, 2010, 20(6): 1078−1091.

[10] GUO La-feng, LI Bao-cheng, ZHANG Zhi-min. Constitutive relationship model of TC21 alloy based on artificial neural network [J]. Transactions of Nonferrous Metals Society of China, 2013, 23(6): 1761−1765.

[11] LI Hong-ying, WEI Dong-dong, LI Yang-hua, WANG Xiao-feng. Application of artificial neural network and constitutive equations to describe the hot compressive behavior of 28CrMnMoV steel [J]. Materials & Design, 2012, 35: 557−562.

[12] SUN Y, ZENG W D, ZHAO Y Q, QI Y L, MA X, HAN Y F. Development of constitutive relationship model of Ti600 alloy using artificial neural network [J]. Computational Materials Science, 2010, 48(3): 686−691.

[13] TAN Ye-fa, HE Long, WANG Xiao-long, HONG Xiang, WANG Wei-gang. Tribological properties and wear prediction model of TiC particles reinforced Ni-base alloy composite coatings [J]. Transactions of Nonferrous Metals Society of China, 2014, 24(8): 2566−2573.

[14] HAN Fei, MO Jian-hua, QI Hong-wei, LONG Rui-fen, CUI Xiao-hui, LI Zhong-wei. Springback prediction for incremental sheet forming based on FEM-PSONN technology [J]. Transactions of Nonferrous Metals Society of China, 2013, 23(4): 1061−1071.

[15] AN Wei-ke, CAI An-hui, LUO Yun, CHEN hua, LIU Wei-xiang, LI Tie-lin, CHEN Min. Optimization of composition of as-cast chromium white cast iron based on wear-resistant performance [J]. Materials & Design, 2009, 30: 2339−2344.

2A97 铝合金时效成形过程中的回弹量和抗拉强度

李红英，鲁晓超

中南大学 材料科学与工程学院，长沙 410083

摘　要：基于正交实验，运用方差分析、多元二次回归和径向人工神经网络研究 2A97 铝合金时效成形过程中的回弹量和抗拉强度。方差分析结果表明，在预弯半径为 400 mm、时效温度为 210 °C 时效 20 h 后试样具有最小的回弹量；而在预弯半径为 1000 mm、时效温度为 180 °C 下时效 15 h 后试样具有最大的抗拉强度。确定了预弯半径、时效温度和时效时间这 3 个因素对试样回弹量和抗拉强度影响大小的顺序。多元二次回归方法和径向人工神经网络的预测结果表明，径向人工神经网络模型具有更高的预测精度。

关键词：铝合金；时效成形；回弹量；抗拉强度；正交试验；人工神经网络

(Edited by Wei-ping CHEN)